Zeeman Study of the Jahn-Teller Effect in the $^3T_{2g}$ State of $Al_2O_3:V^{3+}$ *

P. J. STEPHENS† AND MARIAN LOWE-PARISEAU‡
James Franck Institute, University of Chicago, Chicago, Illinois

(Received 2 February 1968)

The fine structure of the zero-phonon $^3T_{2g}$ state of $Al_2O_3:V^{3+}$ arising from the trigonal field and spin-orbit coupling is anomalously small. Ligand-field theory predicts a 400-cm^{-1} splitting, while the observed levels, first fully identified by Scott and Sturge, span only 14 cm^{-1}. This has been attributed to a large tetragonal Jahn-Teller effect, and a detailed analysis of the zero-phonon levels was made by Scott and Sturge on the basis of Ham's model calculations for octahedral molecules. We have made new measurements on the 0-0 $^3T_{2g}$ band, including the axial spectrum, which shows one σ-polarized transition to be magnetic dipole in origin, and the Zeeman effect of the π and σ spectra at 10°K in fields up to 40 kG parallel and perpendicular to the trigonal axis. The validity of the Ham-Scott-Sturge model has also been further investigated. We have shown that the details of the Scott-Sturge theory require modification, and that it is possible to explain the observed zero-field level pattern within the framework of Ham's general model if, but only if, the assumption of equal quenching of first-order trigonal field and spin-orbit splittings is dropped. In addition, we have obtained values of the first- and second-order trigonal field and spin-orbit coupling energies which reproduce quantitatively the zero-field energies, Zeeman behavior, selection rules, and intensities of all transitions. It is found that the first-order spin-orbit splitting is some four times less quenched than the first-order trigonal-field splitting.

I. INTRODUCTION

THE study of the Jahn-Teller effect in transition-metal complexes has received considerable stimulus from a theoretical paper by Ham.[1] Taking as model examples the orbital triplet states of octahedral molecules, whose vibronic states were discussed by Moffitt and Thorson,[2] Ham investigated the effects of electronic perturbations (such as spin-orbit coupling, external magnetic fields) on the ground vibronic levels in the case where the perturbations are small compared to the Jahn-Teller interaction. It was found that the vibronic coupling causes a marked alteration in the consequences of the perturbations from those predicted in a purely electronic calculation at a fixed, octahedral nuclear configuration. The primary modification consists in a substantial, uniform reduction in the first-order splittings arising from perturbations off-diagonal in the electronic states associated with the various minima of the potential-energy surface. This quenching increases with the Jahn-Teller interaction, becoming total in the limit of the static Jahn-Teller effect, at which point the vibronic states associated with different potential minima do not interact. Second-order effects, involving both higher vibronic levels of the same electronic state and other electronic states of the system, can still be appreciable, however, and can even become dominant when the first-order splittings are very small. A further possible consequence of the Jahn-Teller effect is therefore a radical alteration of the qualitative appearance of the energy levels.

Specific cases of the quenching of first-order splittings by the Jahn-Teller effect have also been encountered in other calculations: for example, McConnell and McLachlan[3] and Child and Longuet-Higgins[4] noted the quenching of electronic orbital angular momentum in $C_6H_6^-$ and X_3, respectively, and Ballhausen[5] showed that spin-orbit splittings can be reduced in square-planar complexes. However, Ham was the first to focus primarily on the manifestations of small perturbations in the presence of large Jahn-Teller interactions and to emphasize their general characteristics.

While most real systems are considerably more complex than the simple cases studied by Ham, it is reasonable to expect, as he pointed out, that their behavior will exhibit qualitatively similar features, and there is now considerable evidence for such effects, relating to a variety of perturbations and systems.[6] One of the clearest examples, and that to be discussed in this paper, was discovered by Scott and Sturge[7] in $Al_2O_3:V^{3+}$, where the V^{3+} ion is coordinated by a trigonally distorted octahedron of O atoms. (This was also the first case to be identified in an excited electronic state.) The low-temperature spectrum of $Al_2O_3:V^{3+}$ had been quite thoroughly studied earlier by Low,[8] Pryce and Runciman,[9] and McClure.[10] While many of

* The support of the Office of Naval Research and of the National Science Foundation is gratefully acknowledged. Equipment grants of the Advanced Research Projects Agency are also acknowledged.

† Present address: Chemistry Department, University of Southern California, Los Angeles, Calif.

‡ Present address: Chemistry Department, Princeton University, Princeton, N.J.

[1] F. S. Ham, Phys. Rev. **138**, A1727 (1965).

[2] W. Moffitt and W. Thorson, Phys. Rev. **108**, 1251 (1957).

[3] H. M. McConnell and A. D. McLachlan, J. Chem. Phys. **34**, 1 (1961).

[4] M. S. Child and H. C. Longuet-Higgins, Phil. Trans. Roy. Soc. London **254A**, 259 (1961).

[5] C. J. Ballhausen, Theoret. Chim. Acta **3**, 368 (1965).

[6] M. D. Sturge, in *Solid State Physics*, edited by F. Seitz, D. Turnbull, and H. Ehrenreich (Academic Press Inc., New York, 1967), Vol. 20, p. 91.

[7] W. C. Scott and M. D. Sturge, Phys. Rev. **146**, 262 (1966).

[8] W. Low, Z. Physik. Chem. (Frankfurt) **13**, 107 (1957).

[9] M. H. L. Pryce and W. A. Runciman, Discussions Faraday Soc. **26**, 34 (1958).

[10] D. S. McClure, J. Chem. Phys. **36**, 2757 (1962).

its features could be understood on the basis of fixed-nuclei ligand-field calculations, the $^3T_{2g}(t_{2g}e_g)$ band was anomalous, showing a pronounced 200-cm.$^{-1}$ vibrational progression (which does not correspond to any known lattice mode[11]) and essentially no trigonal-field or spin-orbit splitting of the lower vibronic levels (the 0-0 band appeared as two components, 8–10 cm^{-1} apart and π and σ polarized, respectively). Pryce and Runciman[9] attributed this to the Jahn-Teller effect and McClure[10] carried out a calculation of the energy levels in the limit of a static tetragonal distortion which supported this hypothesis. In this model, the large tetragonal distortion splits $^3T_{2g}$, the lowest, orbitally nondegenerate component being further slightly split into two levels by second-order spin-orbit coupling. The work of Scott and Sturge[7] showed, however, that the 0-0 band in fact possesses considerable additional structure, three and six transitions being identified in the π and σ polarizations, respectively. This clearly demonstrates that the static limit is not quite attained and that the interaction of the vibronic states belonging to the three distorted tetragonal configurations is still appreciable. The situation is thus of the kind studied by Ham. Scott and Sturge took over Ham's analysis for a T_2 state of an octahedral molecule interacting with a tetragonal (e_g) vibrational mode and applied it directly to the $Al_2O_3:V^{3+}$ situation, assuming that the trigonal field could be treated as a purely electronic perturbation. They concluded that the principal contributors to the observed $^3T_{2g}$ splittings were the trigonal field, its first-order effects quenched by a factor of 40, and second-order spin-orbit coupling to other electronic levels, the first-order spin-orbit splittings being less than the linewidths.

In the course of studying the spectrum of a $Al_2O_3:Co^{3+}$ crystal, we observed some weak lines at $\sim$6300 Å, which were subsequently identified with the 0-0 $^3T_{2g}$ V^{3+} band. The lines were quite sharp, being better resolved than in Scott and Sturge's spectrum. Since the Scott and Sturge paper occupies an important position in the current exploitation of Ham's work, we undertook a study of the Zeeman effect of the lines to confirm their assignment. Some previous Zeeman experiments on this band had been carried out by McClure[12] in fields up to 250 kG but were not interpretable owing to the lack of resolution of the individual lines. With the present crystal we have been able to observe and make a full analysis of the Zeeman effect in magnetic fields up to 40 kG. The results of this study are presented in the following. Magnetic field effects involving excited states thought to be strongly perturbed by Jahn-Teller interactions have previously been observed in $CdS:Co^{2+}$,[13] $Al_2O_3:Cr^{3+}$,[14] and $Co(en)_3^{3+}$ (where en = ethylenediamine).[15] However, no analysis of these results has as yet been published.

II. EXPERIMENTAL

The crystal studied was grown by Linde for Dr. S. A. Marshall of Argonne National Laboratory. Two pairs of parallel plane faces were cut, two faces containing the trigonal (c) axis and 0.97 cm apart, the others perpendicular to the c axis and 1.3 cm separated. Marshall had previously recorded the absorption spectrum of the crystal at liquid-helium temperature with a Cary 14. In addition to the usual features of the $Al_2O_3:Co^{3+}$ spectrum he found a sharp line at 4755 Å. This was attributed by Professor D. S. McClure to the $^1A_{1g}$ absorption band of V^{3+},[9,10] present as an impurity. The crystal was kindly loaned to us by Dr. Marshall to investigate further its Co^{3+} spectrum. In the course of a high-resolution photographic study we not only again observed the 4755 Å line but also found several weaker sharp lines around 6290–6300 Å. These agreed very closely in energy with the components of the $0\rightarrow 0$ $^3T_{2g}$ band of $Al_2O_3:V^{3+}$ reported by Scott and Sturge[7] and confirm the existence of V^{3+} in the crystal. The concentration of V^{3+}, estimated from the intensity of the 6300 Å band and McClure's spectrum[10] is about 5×10^{-2}% by weight.

The Zeeman effect of the $^1A_{1g}$ V^{3+} lines has been studied by Pryce and Runciman[9] and by McClure.[12] We therefore confined our attention to the 6300 Å band. The spectra were taken on a 3.4-m Jarrell-Ash instrument with a 7620-lines-per-inch MIT grating, used in fifth order (excepting Fig. 5, which was obtained with a 30 000-lines-per-inch grating in first order). The light source was a General Electric 150-W tungsten-filament lamp and the absorption was measured photoelectrically, using an EMI 6255B(S13) photomultiplier tube. The magnetic field was provided by a Westinghouse superconducting solenoid, capable of fields up to 50 kG. The crystal was mounted in a cylindrical copper block, machined to fit into the 1.46-in.-diam stainless-steel bore of the magnet, which formed part of the liquid-helium container. Experiments were carried out in which the light passed through the crystal both parallel and perpendicular to the magnetic field. For the latter, a crystal holder was constructed with two mirrors of chromium-plated stainless steel (ferrotype plate) at 45° to the solenoid axis. Polarized spectra were obtained using polaroid-disk polarizers. It was confirmed that the depolarization arising from imperfect orientation of the crystal and mirrors was completely negligible. The resolution was $\sim$0.6 Å$\sim$1.8 cm^{-1} and the spectra were traced at 1.2 Å/min, with a damping time constant of 3 sec. Since the crystal contained so little V^{3+} the absorption was very weak. The major part of the signal at the photomultiplier was therefore biased out and the remainder amplified to give a full-scale

[11] A. S. Barker, Phys. Rev. **132**, 1474 (1963); S. P. S. Porto and R. S. Krishnan, J. Chem. Phys. **47**, 1009 (1967).
[12] D. S. McClure (unpublished).
[13] W. M. Yen and M. D. Sturge, quoted in Ref. 6.
[14] J. Margerie, Compt. Rend. **257**, 2634 (1963); J. Brossel and J. Margerie, in *Paramagnetic Resonance*, edited by W. Low (Academic Press Inc., New York, 1963), Vol. II, p. 535.
[15] R. G. Denning, Chem. Commun. 120 (1967).

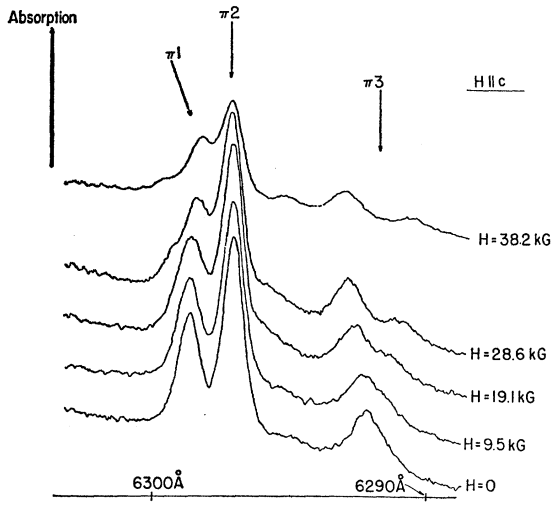

FIG. 1. Traces of experimental spectra: π spectrum, $\mathbf{H} \parallel c$.

deflection on the chart recorder. The noise in our spectra appears to be intrinsic lamp noise. The sloping background is due to changing photomultiplier sensitivity and to Co^{3+} absorption. Spectral calibration was provided by Ne I lines of a Hilger-Watts iron hollow cathode lamp. The temperature of the crystal was not measured. However, the spectrum contains several hot bands originating from a state 8.3 cm^{-1} above the ground state, whose intensities, relative to the cold bands, were measured by Scott and Sturge[7] at 5.2 and 12.6°K. By interpolation, the temperature in our experiments may be put at roughly 10°K.

Our results are portrayed in Figs. 1–6. Note that the traces at different magnetic fields (H), shown in Figs. 1–4, were made at different amplifier gain settings and, consequently, absolute absorption intensity variations with field, cannot be inferred. The σ spectrum with $\mathbf{H} \perp c$, $H=38.2$ kG, is not shown in Fig. 4, as

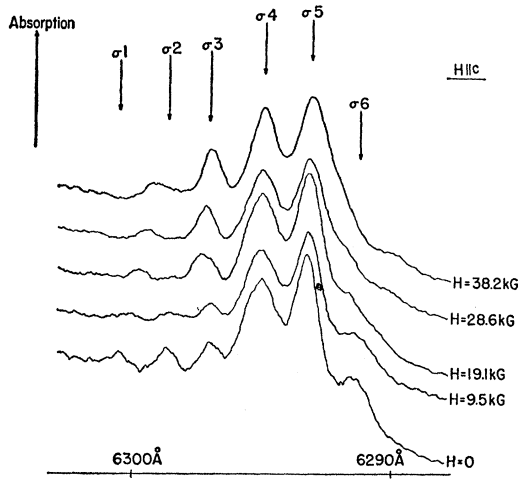

FIG. 2. Traces of experimental spectra: σ spectrum, $\mathbf{H} \parallel c$.

it was run with a different wavelength scale expansion. However, the energies of the transitions are plotted in Fig. 6. The absolute energies given in Fig. 6 are uncertain by ~ 0.5 cm^{-1}. Relative energies are, in optimum cases, accurate to ~ 0.1 cm^{-1}, but the positions of weak bands and shoulders are less precise.[16] Energies are only plotted in Fig. 6 for bands which definitely exist. In some experimental traces indications of other, weak bands are present, but these are not significantly above the noise level and their reality is questionable. The behavior of $\sigma 3$ at the three highest fields $\parallel c$ appears rather anomalous, particularly as $\sigma 3$ and $\pi 2$ are assigned to the same, nondegenerate transition. We attribute the discrepancy to the intrusion of the higher Zeeman component of $\sigma 2$, which, as will be shown later, is expected to lie in this region. The half-height

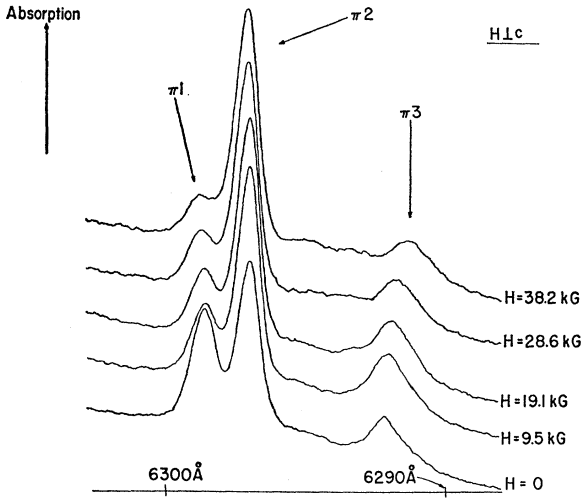

FIG. 3. Traces of experimental spectra: π spectrum, $\mathbf{H} \perp c$ and $\parallel$ to light beam.

widths in zero field are 2–3 cm^{-1} excepting $\sigma 4$, which is ~ 4 cm^{-1} broad.

The σ and π spectra at zero field are qualitatively identical to those published by Scott and Sturge.[7] The agreement of the transition energies is good in all cases but one. The exception is the $\sigma 6$ line, which we find to lie above $\sigma 4$ by 9.0 cm^{-1}—appreciably more than the 8.3-cm^{-1} separation given by Scott and Sturge. The significance of this observation will be discussed later. The zero-field axial spectrum (Fig. 5) was not reported by Scott and Sturge. It is almost identical to the σ spectrum but differs by the absence of $\sigma 3$. This shows that the major part of the observed intensity (specifically, that in $\sigma 1$, $\sigma 4$, $\sigma 5$, $\sigma 6$, $\pi 2$, and $\pi 3$) is electric dipole, but that $\sigma 3$ is a parallel-polarized magnetic dipole transition. The hot band to level 2

[16] The asymmetry of many of the lines adds to the uncertainty in their positions. Wavelengths were obtained by averaging the mean wavelength of a line over its whole height; these values often differed appreciably from the peak wavelengths.

appears in all three spectra and the electric and magnetic dipole strengths of this transition therefore can not be fully determined experimentally. However, since $\pi 1$ is considerably stronger than $\sigma 2$ (by a factor of 5 according to Scott and Sturge) and the intensity in the corresponding axial band is comparable to $\sigma 2$, $\pi 1$ can definitely be assigned as a predominantly parallel-polarized electric dipole transition.

III. ANALYSIS

A "complete" d-electron calculation has been carried out for $Al_2O_3:V^{3+}$ by Macfarlane[17] and accounts satisfactorily for the extensive spectroscopic and magnetic data available, excepting the fine structure of the $^3T_{2g}$ band. The values of the cubic-field, trigonal-field, electron-repulsion, and spin-orbit coupling parameters obtained, and the fine structure of the ground

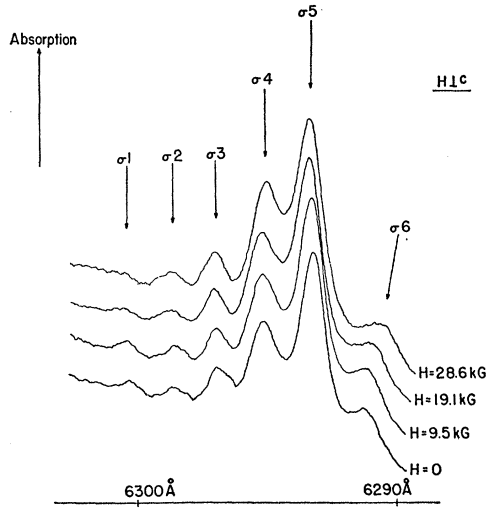

FIG. 4. Traces of experimental spectra: σ spectrum, $\mathbf{H} \perp c$ and $\parallel$ to light beam.

$^3T_{1g}(t_{2g}^2)$ and the $^3T_{2g}(t_{2g}e_g)$ levels calculated therefrom, are shown in Fig. 7. The states are classified according to the C_3 site symmetry.[10] The zero-field splitting of the ^3A ground state has been measured both by paramagnetic resonance techniques[18] and by optical spectroscopy.[7,19] The most recent value is 8.3 cm^{-1}. This agrees well with the calculated value and we shall adopt this figure in the following discussion.

The 6300 Å band is assigned to the zero-phonon transition to the $^3T_{2g}$ level.[10] Scott and Sturge[7] determined the temperature dependence of the various transitions and thereby showed $\pi 1$, $\sigma 1$, $\sigma 2$, and $\sigma 4$ to be hot bands, originating in the higher ^3A component. Making use of this information and taking the ^3A zero-field splitting to be 8.3 cm^{-1}, the structure of the

[17] R. M. Macfarlane, J. Chem. Phys. **40**, 373 (1964).
[18] S. Foner and W. Low, Phys. Rev. **120**, 1585 (1960).
[19] S. Sakatsume and I. Tsujikawa, J. Phys. Soc. Japan **19**, 1080 (1964).

FIG. 5. Traces of experimental spectra: axial spectrum, $H=0$. The arrow indicates the location of $\sigma 3$ in the σ spectrum.

upper state can be deduced from the spectrum. This is shown in Fig. 8, together with the assignments of the observed bands. Some uncertainty exists in the assignment of the $\sigma 4$ and $\sigma 6$ transitions. Scott and Sturge, on the basis of their measured 8.3-cm^{-1} separation, assigned $\sigma 4$ to the hot band corresponding to the cold $\sigma 6$ transition. However, as noted earlier, we find them to be $\sim$9.0 cm^{-1} apart. There are two ways of explaining our result: either the upper state of $\sigma 4$ is not that of $\sigma 6$, but another state slightly lower in energy; or, the $\sigma 4$ band is in fact a composite of two hot bands, of energies respectively higher and lower than 15881.2 cm^{-1}, that corresponding to $\sigma 6$ being the higher in energy. We believe the latter to be the case and that the lower component of $\sigma 4$ is the partner of the cold $\pi 3$ transition. The abnormally large width of $\sigma 4$, already mentioned, is initial evidence for this interpretation. Further support will be provided below by the Zeeman-effect data and the theoretical study. This assignment is adopted in Fig. 8 and the energy of the highest $^3T_{2g}$ level is hence taken from the $\sigma 6$ transition. In all other respects, Fig. 8 is essentially identical to the analogous diagram (Fig. 4) of Scott and Sturge.

We now wish to determine the effects of magnetic fields on these levels. The behavior of the ground ^3A

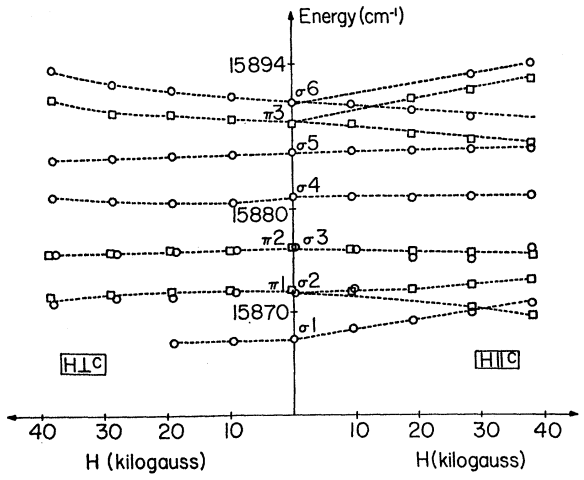

FIG. 6. Transition energies. Squares and circles denote π- and σ-polarized transitions, respectively. $\pi 1$, $\sigma 1$, $\sigma 2$, and $\sigma 4$ are hot bands

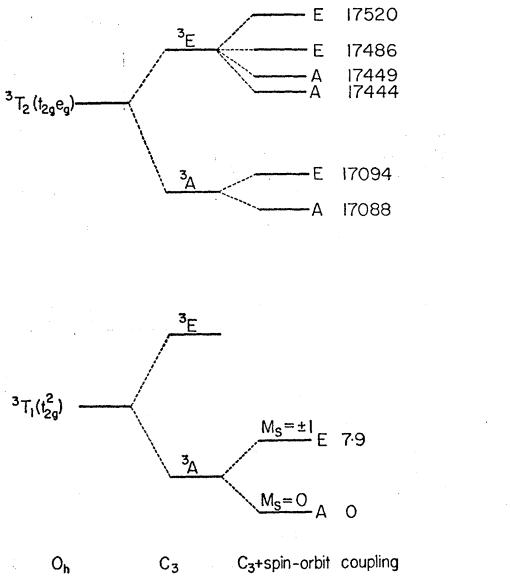

FIG. 7. Electronic states of $Al_2O_3:V^{3+}$ deriving from $^3T_{1g}(t_{2g}^2)$ and $^3T_{2g}(t_{2g}e_g)$ O_h levels. Energies are those calculated by Macfarlane with $\Delta=18\,000$, $B=610$, $C=2500$, $v=800$, $v'=200$, and $\zeta=155$ (all in cm^{-1}). M_S values refer to the trigonal axis and are appropriate to a pure ^3A state.

state in magnetic fields has been studied by paramagnetic resonance,[18,20,21] magnetic-susceptibility measurements,[22] and through the Zeeman effect of the sharp, intraconfigurational transition to the $^1A_{1g}$ state.[9,12] The energies with the field $||$ and $\perp$ to the trigonal axis, calculated[23] using $g_{||}=1.915$ [20] and $g_\perp=1.725$,[22] are plotted in Fig. 9. From these, the Zeeman pattern of the zero-phonon $^3T_{2g}$ level can be deduced, as is also shown in Fig. 9. The cold bands furnish the behavior of levels 1, 3, 4, and 5. Level 2 can only be studied through the $\pi1$ and $\sigma2$ hot bands. From the $\pi1$ transition, there are two possibilities for the splitting in fields $||$ c, as shown in Fig. 9. The field dependence of $\sigma2$ is not clearly observed and the alternatives cannot be unambiguously distinguished. However, if the smaller splitting is chosen, the upper Zeeman component of $\sigma2$ can lie $\sim$15876 cm^{-1} at 30–40 kG. This is close to the position of $\sigma3$ and enables the observed anomalous behavior of $\sigma3$ (noted above) to be explained.[24] This is not possible with the larger splitting. The effect of fields $\perp$ c on level 2 is also uncertain without assumptions about selection rules. The range of possibilities is therefore indicated in Fig. 9. We should note that when a transition does not split observably in the field, the energies given in Figs. 6 and 9 are averages over the Zeeman components. This is particularly relevant to the $\mathbf{H}\perp c$ spectra, where no splittings are resolved.

From the level scheme thus extracted, the behavior of the $\sigma1$ and $\sigma4$ hot bands may be predicted and the validity of their assignments tested. The splitting of $\sigma1$ with $\mathbf{H}$ $||$ c is in quantitative agreement with that predicted from $\pi2$ and $\sigma3$. Only the upper Zeeman component is expected to be seen because of the depopulation of the $M_s=+1$ ^3A level by the Zeeman splitting. The absence of an observable splitting of $\sigma4$ with $\mathbf{H}$ $||$ c shows that the splitting of the excited state (or states) is approximately equal to that of the ^3A $M_s=\pm1$ states. This is consistent with the upper state being either of level 4 or 5, or both, since levels 4 and 5 have similar Zeeman splittings, and therefore with the assignments of Fig. 8. From an experimental standpoint, the possibility of there being a new state, unobserved in other transitions, is not ruled out by the Zeeman effect data. However, we shall show subsequently that this assignment is unlikely theoretically and it is excluded from Fig. 9. The shift of $\sigma4$ in fields $\perp c$ is smaller than expected on the basis of $\sigma6$ and about that predicted from $\pi3$. However, since the Zeeman components are unresolved and the relative transition probabilities will be different in the hot and cold bands, this does not invalidate our earlier assignment of $\sigma4$.

Further information about the $^3T_{2g}$ levels is obtainable from the spectra if the ground and excited states can be assigned to single irreducible representations of the C_3 group. This will be possible as long as the static Jahn-Teller limit is not reached in the excited state. As already mentioned, the existence of the fine structure indicates that the static limit is not attained. We shall therefore assign the upper state symmetries within C_3. The ground ^3A levels are A and E. Selection rules for electric and magnetic dipole transitions are the same: $A\rightarrow A$, $A\rightarrow E$, and $E\rightarrow A$ transitions are $||$, $\perp$, and $\perp$

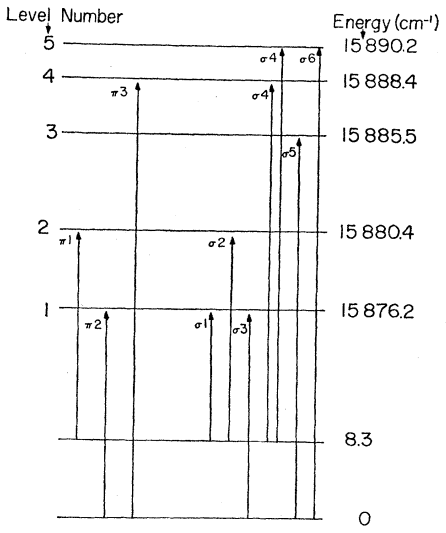

FIG. 8. Zero-field energy levels and transitions.

[20] G. M. Zverev and A. M. Prokhorov, Zh. Eksperim. i Teor. Fiz. **38**, 449 (1960) [English transl.: Soviet Phys.—JETP **11**, 330 (1960)].
[21] J. Lambe and C. Kikuchi, Phys. Rev. **118**, 71 (1960).
[22] C. R. Quade, W. H. Brumage, and C. C. Lin, J. Chem. Phys. **37**, 1368 (1962).
[23] See Ref. 17 for general expressions for the magnetic field energies.
[24] This assignment also requires a reversal of selection rules from π to σ polarization. See below.

polarized, respectively; $E\rightarrow E$ transitions may occur in both polarizations. The $^3T_{2g}$ states in zero field are then identified as follows:

$$1:A,\quad 2:E,\quad 3:E,\quad 4:A,A,\quad 5:E.$$

The degeneracy of level 4 is accidental and not group theoretical. The assignment of level 2 as an E state, rather than an accidental doublet, follows from the existence of parallel-polarized intensity in $\pi 1$ (see Sec. II). Note that the selection-rule arguments identify a degeneracy in level 3 which is not observed directly through a Zeeman splitting. The use of C_3 is consistent with all of the data.[25]

For E states which split observably in fields $\| c$ and which participate in hot bands, the symmetries of the individual Zeeman components can also be assigned, since a magnetic field along the trigonal axis does not lower the symmetry below C_3. Defining E_+ and E_- as the nondegenerate representations of C_3 transforming like $S=1$, $M_S=+1$, and -1 functions, we have the following selection rules:

$$\begin{array}{cc} \| & \perp \\ E_+\rightarrow E_+, & E_+\rightarrow E_-, \\ \| & \perp \\ E_-\rightarrow E_-, & E_-\rightarrow E_+. \end{array}$$

From Fig. 9 we then infer that for levels 2 and 5 $E_-<E_+$ and $E_+<E_-$, respectively. The C_3 selection rules are consistent with our interpretation of the Zeeman behavior of $\sigma 2$ (see Ref. 24).

In summary, the structure of the zero-phonon $^3T_{2g}$ level of $Al_2O_3:V^{3+}$ bears no resemblance to that predicted by Macfarlane's purely electronic calculation. The Zeeman experiments unambiguously identify eight excited states and can be satisfactorily interpreted without postulating more. The assumption of C_3 selection rules extends this number to nine, level 3 being degenerate but not observably split at 40 kG.

IV. THEORY

The evolution and current status of ideas on the "anomalous" structure of the $^3T_{2g}$ $Al_2O_3:V^{3+}$ state were summarized in Sec. I. It appears to be well established that a dynamic Jahn-Teller effect involving a basically tetragonal distortion of the VO_6 octahedron is to be held responsible. Interaction with a trigonal mode can be excluded, as this would not quench the trigonal-field splitting.[1] Accepting this, it then remains to calculate the spin-orbit and trigonal-field structure of the zero-phonon level. Here, one may either attempt an *a priori* treatment, involving an analysis of the proper vibrational modes associated with the V^{3+} impurity in the corundum lattice, or adopt a phenomenological approach, searching for a semiempirical Hamiltonian which reproduces the observed energy levels. In view of the general complexity of the former, the latter procedure was recommended by Ham and was that followed by Scott and Sturge. In the subsequent discussion we shall explore its applicability to the Zeeman experiments. Before the effects of magnetic fields can be considered, however, the zero-field structure must be accounted for. To start with, therefore, we shall follow through the analysis propounded by Scott and Sturge. This in turn must be prefaced by a resumé of the relevant results derived by Moffitt and Thorson and by Ham, on which it is based.

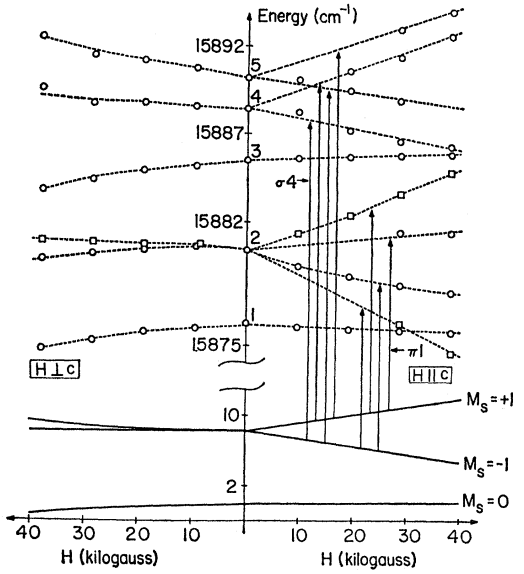

FIG. 9. Zeeman patterns of ground and excited levels. Squares and circles emanating from excited level 2 show different possibilities consistent with the observed $\pi 1$ behavior. Vertical lines indicate observed selection rules for Zeeman components of hot bands. M_S values refer to the trigonal axis and are appropriate to a pure ^3A state.

The dynamic Jahn-Teller effect of a T_2 electronic state of an octahedral MX_6 molecule interacting with an e_g vibrational mode was first treated by Moffitt and Thorson.[2] They assumed the molecular Hamiltonian to be of the form

$$\mathcal{H}=\mathcal{H}_{el}^{(0)}+\mathcal{H}_{vib}^{(0)}+\mathcal{H}_{JT}^{(1)}+\mathcal{H}^{(2)}, \qquad (1)$$

where $\mathcal{H}_{el}^{(0)}$ and $\mathcal{H}_{vib}^{(0)}$ are the zeroth-order electronic and vibrational Hamiltonians, the latter taken to be harmonic, the Jahn-Teller interaction $\mathcal{H}_{JT}^{(1)}$ is small compared to $\mathcal{H}_{el}^{(0)}$, and $\mathcal{H}^{(2)}$ comprises terms smaller than $\mathcal{H}_{JT}^{(1)}$. Situations in which $\mathcal{H}$ contains other terms of the same order of magnitude as $\mathcal{H}_{JT}^{(1)}$ are more complex and were not considered. In particular, the spin-orbit interaction $\mathcal{H}_{so}$ is supposed either larger than $\mathcal{H}_{JT}^{(1)}$, when it is included in $\mathcal{H}_{el}^{(0)}$ and already taken account of in the T_2 state, or smaller than $\mathcal{H}_{JT}^{(1)}$, in which case it enters into $\mathcal{H}^{(2)}$ and T_2 is a $(2S+1)$-fold degenerate spin multiplet. In addition, $\mathcal{H}_{JT}^{(1)}$ was restricted to terms linear in the e_g nuclear coordinates Q_θ and Q_ϵ, $\mathcal{H}^{(2)}$ ignored, and mixing of

[25] This would not be the case if all intensity were assumed to be electric dipole in origin, since then the cold transition to level 1 would be both $\|$ and $\perp$ polarized.

different eigenstates of $\mathcal{H}_{el}^{(0)}$ by $\mathcal{H}_{JT}^{(1)}$ neglected. For the ${}^3T_{2g}$ V^{3+} state under consideration here, $\mathcal{H}_{JT}^{(1)} > \mathcal{H}_{so}$; for brevity, we therefore present our discussion in terms of this case, and quote results specifically for a ${}^3T_{2g}$ state.

Within this framework the potential-energy surfaces in Q_θ, Q_ϵ space (depicted by Sturge[26]) are the sum of three paraboloids which intersect at the undisplaced octahedral configuration. The three minima correspond to tetragonal distortions along the fourfold axes of the octahedron; they lie at $\Delta E = l^2/2\mu\omega^2$ below the energy of the undistorted geometry E_0, l being a parameter specifying the strength of the Jahn-Teller interaction and μ and ω being, respectively, the effective mass and the angular frequency of the e_g vibration. ΔE is referred to as the Jahn-Teller energy; in a stable tetragonal configuration the separation of the energy surfaces is $3\Delta E$ (the upper surfaces being twofold degenerate at this point). Each paraboloid surface corresponds to one of three real ${}^3T_{2g}$ components, conventionally labelled ξ, η, and ζ (Griffith's notation[27]), and each is threefold spin degenerate.

The solutions of the dynamic vibronic problem turn out to be simple products of the form

$$\Psi_{iM_S n_\theta n_\epsilon} = \psi_{iM_S}(\tau)\chi_{in_\theta n_\epsilon}(Q_\theta, Q_\epsilon), \tag{2}$$

of energy

$$E_{T_{2n_\theta n_\epsilon}} = E_0 - l^2/2\mu\omega^2 + (n_\theta + n_\epsilon + 1)\hbar\omega; \tag{3}$$

i and M_S specify ${}^3T_{2g}$ orbital and spin states, respectively. The function ψ_{iM_S} depends on electronic coordinates τ, and in the lowest-order approximation, is independent of nuclear geometry. The vibrational function $\chi_{in_\theta n_\epsilon}$ is a solution of the two-dimensional harmonic-oscillator problem for the potential surface corresponding to the ith T_2 state; it is independent of M_S. n_θ and n_ϵ are the quantum numbers of the specific vibrational level. The ground vibronic state comprises the functions $\Psi_{\xi M_S 00}$, $\Psi_{\eta M_S 00}$, and $\Psi_{\zeta M_S 00}$, M_S being allowed three values. The closest excited levels lie $\hbar\omega$ higher in energy. The simplicity of the eigenfunctions is rather exceptional in Jahn-Teller problems; it arises because the vibronic interaction is diagonal in the ξ, η, ζ representation for *all* vibrational displacements.

The work of Moffitt and Thorson was extended by Ham[1] to include the $\mathcal{H}^{(2)}$ terms of Eq. (1). As noted earlier, if $\mathcal{H}$ contains other terms comparable in magnitude to $\mathcal{H}_{JT}^{(1)}$, the vibronic problem can become extremely complicated. However, when $\mathcal{H}_{JT}^{(1)} \gg \mathcal{H}^{(2)}$, $\mathcal{H}^{(2)}$ can be adequately treated by perturbation theory. Ham evaluated the effects of a variety of electronic perturbations satisfying this condition on the ground vibronic state up to second order in perturbation theory. Within the ground vibronic manifold, the matrix elements of a purely electronic operator $\mathcal{O}$ are given by

$$\langle iM_S 00 \mid \mathcal{O} \mid jM_S' 00\rangle = \langle \psi_{iM_S} \mid \mathcal{O} \mid \psi_{jM_S'}\rangle \langle \chi_{i00} \mid \chi_{j00}\rangle. \tag{4}$$

In the harmonic approximation,

$$\langle \chi_{i00} \mid \chi_{j00}\rangle = \exp(-3\Delta E/2\hbar\omega) \qquad (i \neq j),$$
$$\langle \chi_{i00} \mid \chi_{i00}\rangle = 1, \tag{5}$$

and

$$\langle iM_S 00 \mid \mathcal{O} \mid jM_S' 00\rangle = \langle \psi_{iM_S} \mid \mathcal{O} \mid \psi_{jM_S'}\rangle \times \exp(-3\Delta E/2\hbar\omega) \qquad (i \neq j),$$
$$\langle iM_S 00 \mid \mathcal{O} \mid iM_S' 00\rangle = \langle \psi_{iM_S} \mid \mathcal{O} \mid \psi_{iM_S'}\rangle. \tag{6}$$

The matrix elements of $\mathcal{O}$ which are off-diagonal in the ξ, η, ζ representation are thus reduced below the value obtained in a purely electronic calculation ($\langle \psi_{iM_S} \mid \mathcal{O} \mid \psi_{jM_S'}\rangle$) by a quenching factor independent of i and j and depending exponentially on ΔE. Physically this is due to the reduced overlap of the vibrational functions associated with different potential minima arising from their relative displacement in Q_θ, Q_ϵ space. On the other hand, diagonal matrix elements are not quenched. As a result, if a perturbation is wholly off-diagonal,[28] the effect of the Jahn-Teller interaction is to uniformly quench its first-order splitting of the ground vibronic state by the factor $\exp(-3\Delta E/2\hbar\omega)$. The orbital angular momentum, orbital Zeeman interaction, and spin-orbit coupling operators $\mathbf{L}$, $\beta\mathbf{L}\cdot\mathbf{H}$, and $\mathcal{H}_{so}$ are important examples of such off-diagonal operators. Conversely, the first-order effects of a totally diagonal operator, such as the spin Zeeman interaction $2\beta\mathbf{S}\cdot\mathbf{H}$, are unaffected.

The second-order effects of $\mathcal{H}^{(2)}$ depend on sums of the form

$$\langle iM_S 00 \mid \mathcal{H}^{(2)}\mathcal{H}^{(2)} \mid jM_S' 00\rangle = \sum_{\alpha \neq T_2 00} \frac{\langle iM_S 00 \mid \mathcal{H}^{(2)} \mid \alpha\rangle\langle \alpha \mid \mathcal{H}^{(2)} \mid jM_S' 00\rangle}{E_{T_2 00} - E_\alpha}. \tag{7}$$

These can be divided into two parts: in the first, α is a member of the ${}^3T_{2g}$ vibronic manifold; in the second are included all contributions from other electronic states. Matrix elements in the first class—henceforth referred to as in-state terms—are zero for diagonal operators and, for off-diagonal operators, reduce to

$$\langle iM_S 00 \mid \mathcal{O}\mathcal{O}' \mid jM_S' 00\rangle = -(\hbar\omega)^{-1} G\left(\frac{3\Delta E}{2\hbar\omega}\right) \times [\exp(-3\Delta E/\hbar\omega)] \sum_{k \neq i,j;M_S''} \langle \psi_{iM_S} \mid \mathcal{O} \mid \psi_{kM_S''}\rangle \times \langle \psi_{kM_S''} \mid \mathcal{O}' \mid \psi_{jM_S'}\rangle \qquad (i \neq j),$$
$$\langle iM_S 00 \mid \mathcal{O}\mathcal{O}' \mid iM_S' 00\rangle = -(\hbar\omega)^{-1} G\left(\frac{3\Delta E}{\hbar\omega}\right) \times [\exp(-3\Delta E/\hbar\omega)] \sum_{k \neq i;M_S''} \langle \psi_{iM_S} \mid \mathcal{O} \mid \psi_{kM_S''}\rangle \times \langle \psi_{kM_S''} \mid \mathcal{O}' \mid \psi_{iM_S'}\rangle, \tag{8}$$

[26] M. D. Sturge, Phys. Rev. **140**, A880 (1965).

[27] J. S. Griffith, *The Theory of Transition-Metal Ions* (Cambridge University Press, Cambridge, 1961).

[28] Here and in the following discussion we use the terms "diagonal" and "off-diagonal" in the restricted context of the real, orbital T_2 representation. When we wish to imply complete diagonality within the whole ${}^3T_{2g}$ basis we shall use the phrase "truly diagonal."

where

$$G(X)=\sum_{n=1}^{\infty}\frac{X^n}{n\times n!}.$$

In the limit of $X\to\infty$, $G(X)\to e^X/X$. Hence, for large Jahn-Teller effects, the off-diagonal elements vary as $(\Delta E)^{-1}\exp(-3\Delta E/2\hbar\omega)$ while the diagonal terms become

$$\langle iM_S00\mid \mathcal{O}\mathcal{O}'\mid iM_S'00\rangle=-(3\Delta E)^{-1}\times\sum_{k\neq i;M_S''}\langle\psi_{iM_S}\mid\mathcal{O}\mid\psi_{kM_S''}\rangle\langle\psi_{kM_S''}\mid\mathcal{O}'\mid\psi_{iM_S'}\rangle. \quad (9)$$

The latter may still be appreciable when the former are essentially completely quenched. The remaining, out-of-state terms can be simplified if the other electronic states Γ are far enough removed to put $E_{T_200}-E_\alpha\approx E_{T_2}-E_\Gamma$, where E_Γ is the same for all vibronic levels of Γ.[29] If Γ is not subject to a Jahn-Teller interaction, we can write $\mid\alpha\rangle=\psi_\gamma(\tau)\chi_n(Q_\theta,Q_\epsilon)$, where γ specifies the component of Γ and n is a vibrational quantum number. If such interactions are present, within the framework of the Moffitt-Thorson theory, $\mid\alpha\rangle=\sum_{\gamma,n}C_{\alpha\gamma n}\psi_\gamma\chi_n$. In either case, since the $C_{\alpha\gamma n}$ coefficients define a unitary transformation, the contribution of the state Γ becomes

$$\langle iM_S00\mid\mathcal{O}\mathcal{O}'\mid jM_s'00\rangle=\sum_\gamma\left\{\frac{\langle\psi_{iM_S}\mid\mathcal{O}\mid\psi_\gamma\rangle\langle\psi_\gamma\mid\mathcal{O}'\mid\psi_{jM_S'}\rangle}{E_{T_2}-E_\Gamma}\left[\sum_n\langle\chi_{i00}\mid\chi_n\rangle\times\langle\chi_n\mid\chi_{j00}\rangle\right]\right\}. \quad (10)$$

Since χ_n forms a complete set, the second sum can be contracted, giving

$$\langle iM_S00\mid\mathcal{O}\mathcal{O}'\mid jM_S'00\rangle=\left\{\sum_\gamma\langle\psi_{iM_S'}\mid\mathcal{O}\mid\psi_\gamma\rangle\frac{\langle\psi_\gamma\mid\mathcal{O}'\mid\psi_{jM_S'}\rangle}{E_{T_2}-E_\Gamma}\right\}\times\langle\chi_{i00}\mid\chi_{j00}\rangle. \quad (11)$$

The vibrational overlap integrals of Eq. (11) are just those occurring in the first-order matrix elements of Eq. (4) and, in analogous fashion, $\langle iM_S00\mid\mathcal{O}\mathcal{O}'\mid iM_S'00\rangle$ is not affected by the Jahn-Teller interaction but $\langle iM_S00\mid\mathcal{O}\mathcal{O}'\mid jM_S'00\rangle$ is quenched by $\exp(-3\Delta E/2\hbar\omega)$.

In both types of second-order term, therefore, off-diagonal elements decrease exponentially with increasing ΔE while diagonal elements decrease either as $(\Delta E)^{-1}$ or not at all. Hence, for an off-diagonal electronic operator, the diagonal second-order elements are the only significant terms remaining to second order in the perturbation theory in the case of a large Jahn-Teller effect; in this limit the static Jahn-Teller effect is reached. As Ham pointed out,[1] in the static limit the second-order terms are just those calculated in a purely electronic calculation for the lowest T_2 component in a distorted tetragonal configuration, the upper T_2 components being taken to be $3\Delta E$ higher in energy.

For the perturbation approach to be valid, $\mathcal{H}^{(2)}\ll\mathcal{H}_{JT}^{(1)}$ is required. In this case, the splittings due to $\mathcal{H}^{(2)}$ are then much less than the separation of the vibronic levels $\hbar\omega$. Note also that the dominance of second-order over first-order effects in or near the static limit does not mean a breakdown of perturbation theory. Rather, the first-order terms are just "accidentally" small.

Returning now to the $Al_2O_3:V^{3+}$ spectrum, we may first note that the splitting of the zero-phonon $^3T_{2g}$ level is 14 cm^{-1} compared to a progression interval of 200 cm^{-1}. This clearly points to a situation of the type discussed by Ham and justifies a perturbation treatment of the splittings. Scott and Sturge then made the basic assumptions that the trigonal field could be treated as a purely electronic perturbation $\mathcal{H}_{TF}$, and the Moffitt-Thorson-Ham results directly taken over. These are radical simplifications of the real problem: The trigonal field arises from a distortion of the V^{3+} environment from octahedral and this must affect the vibrational motions of the neighboring atoms too; also, the VO_6 complex cannot properly be isolated from the surrounding matrix. The central purpose of the present paper is to investigate their validity.

The matrices of $\mathcal{H}_{so}$ and $\mathcal{H}_{TF}$ within the $^3T_{2g}$ electronic states are given in Fig. 10 [see part (a) of caption]. ζ and v are the conventional spin-orbit and trigonal-field parameters. The basis states are defined with respect to cubic axes and we have adopted real spin functions, labelled by and transforming like x, y, and z. The trigonal axis is taken along the cubic 111 direction. Under $\mathcal{H}_{so}$ alone, $^3T_{2g}$ splits into A_2, E, T_1, and T_2 states, with first-order energies $-\frac{1}{2}\zeta$, $\frac{1}{4}\zeta$, $\frac{1}{4}\zeta$, and $-\frac{1}{4}\zeta$; $\mathcal{H}_{TF}$ by itself gives rise to ^3A and ^3E states of energies $-\frac{1}{3}v$ and $+\frac{1}{6}v$. The ζ and v values for $Al_2O_3:V^{3+}$ obtained by Macfarlane from his ligand-field calculation and available spectroscopic and magnetic data were 160 and 860 cm^{-1}, respectively.[30] The first-order $^3T_{2g}$ structure obtained with these parameters is shown in Fig. 11(a). In the presence of a Jahn-Teller effect larger than $\mathcal{H}_{so}$ and $\mathcal{H}_{TF}$, however, the first-order matrix within the ground vibronic state becomes that shown in Fig. 10 [part (b) of caption], and the splittings are reduced, since both operators are off-diagonal. As the observed spread in energy is 14 cm^{-1}, the quenching factor is in the range 0.1–0.01. Scott and Sturge concluded on the basis of selection rule arguments that the observed states can be divided into levels 1 and 2 and levels 3–5, the two sets deriving respectively from ^3A and ^3E states, 9 cm^{-1} apart. This leads to a quenching factor of 0.023 and, with $\hbar\omega=200$ cm^{-1}, to a Jahn-Teller energy $\Delta E=503$ cm^{-1}.

[29] This is essentially the criterion for the validity of the first-order Moffitt-Thorson theory.

[30] These values are slightly different from those used in Fig. 7; see Ref. 15 of Ref. 17.

ξx	ξy	ξz	ηx	ηy	ηz	ζx	ζy	ζz	
a	g	-g+h	b+c	d+e	f	b+c	f	d+e	ξx
		g+h	-d	b+c	-f	-f	b+c	f	ξy
			-f	f	b+c	-d	-f	b+c	ξz
				g	-g+h	b+c	-f	f	ηx
				a	g+h	f	b+c	d+e	ηy
						-f	-d	b+c	ηz
							g	-g+h	ζx
								g+h	ζy
								a	ζz

FIG. 10. Trigonal-field, spin-orbit coupling, and magnetic-field matrices. (a) First-order electronic matrix:

$b=-\frac{1}{6}v(-143.3)$, $d=-\frac{1}{4}\zeta(-40)$, $a=c=e=f=g=h=0$;

(b) first-order Jahn-Teller matrix:

$$b=-\tfrac{1}{6}v\exp(-3\Delta E/2\hbar\omega)(-3.31),$$
$$d=-\tfrac{1}{4}\zeta\exp(-3\Delta E/2\hbar\omega)(-0.92),$$
$$a=c=e=f=g=h=0;$$

(c) in-state second-order Jahn-Teller matrix:

$$a=-(\zeta^2/16\hbar\omega)G(3\Delta E/\hbar\omega)[\exp(-3\Delta E/\hbar\omega)](-1.26),$$
$$c=-(v^2/36\hbar\omega)G(3\Delta E/2\hbar\omega)[\exp(-3\Delta E/\hbar\omega)](-0.81),$$
$$e=-(\zeta^2/16\hbar\omega)G(3\Delta E/2\hbar\omega)[\exp(-3\Delta E/\hbar\omega)](-0.06),$$
$$f=-(\zeta v/24\hbar\omega)G(3\Delta E/2\hbar\omega)[\exp(-3\Delta E/\hbar\omega)](-0.23),$$
$$b=d=g=h=0;$$

(d) out-of-state second-order Jahn-Teller matrix:

$$a\neq 0,\quad b=c=d=e=f=g=h=0;$$

(e) semiempirical matrix:

$$a=x\quad b+c=t,\quad d=-s,\quad e=f=g=h=0;$$

(f) magnetic field matrices:

$\mathbf{H}\,||\,c$: $g=-(2i\beta H/\sqrt{3})(-0.054i/\text{kG})$, $a=b=c=d=e=f=h=0$;
$\mathbf{H}\perp c$: $h=-\sqrt{2}i\beta H(-0.066i/\text{kG})$, $a=b=c=d=e=f=g=0$;

values in parentheses (all in cm^{-1}) evaluated with

$\zeta=160\ \text{cm}^{-1}$, $v=860\ \text{cm}^{-1}$, $3\Delta E/2\hbar\omega=3.77$,
$\hbar\omega=200\ \text{cm}^{-1}$,

and

$\beta=0.0467\ \text{cm}^{-1}/\text{kG}$.

The level pattern is then as shown in Fig. 11(b). The largest spin-orbit splitting, that of the ^3E state, is $\sim 2\ \text{cm}^{-1}$ and hence on the order of the linewidths. As a result, Scott and Sturge concluded that first-order spin-orbit effects were not resolved.

The additional splittings observed could therefore be attributed only to second-order effects. In-state contributions can be evaluated from Eq. (8) and comprise terms second order in $\mathcal{H}_{SO}$, second order in $\mathcal{H}_{TF}$, and cross terms; all are shown in Fig. 10 [part (c) of caption]. Numerical values obtained with Macfarlane's parameters, $\hbar\omega=200\ \text{cm}^{-1}$ and $3\Delta E/2\hbar\omega=3.77$ from the first-order quenching factor, are also given. The result of then diagonalizing the first-order and in-state second-order matrices together is portrayed in Fig. 11(c). The second-order trigonal field matrix is formally identical to the first-order matrix and hence does not give rise to any further splittings. Of the other terms, the diagonal second-order spin-orbit coupling elements are by far the largest, and, further, are larger than the off-diagonal first-order terms. However, even these are clearly still too small to explain the remaining observed 4–5-cm^{-1} splittings.

It is therefore necessary to go on to consider out-of-state second-order effects. Since off-diagonal terms are quenched equally to first-order terms, these can be ignored.[31] The diagonal terms must be identical in form to the diagonal in-state terms apart from an irrelevant constant, truly diagonal matrix. As shown in Fig. 10 [part (d) of caption], therefore, only terms of second order in $\mathcal{H}_{SO}$ contribute. In the absence of other contributions, the diagonal second-order spin-orbit coupling

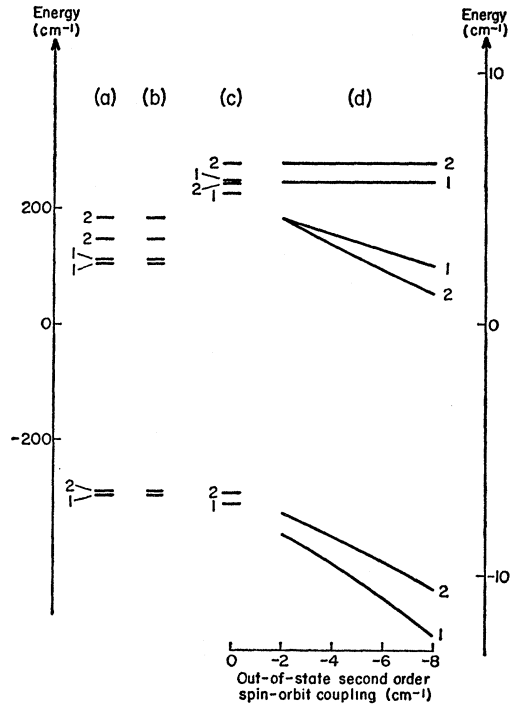

FIG. 11. Energy levels calculated from matrices of Fig. 10. (a) Part (a) of caption; (b) part (b); (c) parts (b) and (c); (d) parts (b), (c), and (d) together. The left energy scale applies to part (a) of this figure; the right, to parts (b)–(d). Numbers indicate degeneracy.

[31] These terms can be estimated by comparing Macfarlane's complete calculation of the $^3T_{2g}$ levels to a first-order calculation (with the same parameters) and reducing the difference (which measures the second-order effects) by 0.023.

terms split the ground vibronic state into a triplet and a sextet, comprising the functions ξx, ηy, ζz and ξy, ξz, ηx, ηz, ζx, ζy, respectively. In each triplet function the spin component is quantized along the distortion axis corresponding to the orbital state; in the sextet functions the spins are perpendicular to this axis. This situation is actually reached in the static limit, the case discussed by McClure.[10]

It is hard to calculate the second-order contributions of other electronic states accurately. Scott and Sturge quote an estimate by Baltzer of the total spin-orbit splitting in the static limit, giving 2–7 cm^{-1}, the triplet state being lowest. Since the in-state contribution [given by Eq. (9)] is 1.06 cm^{-1}, this puts the out-of-state part at 1–6 cm^{-1}. Scott and Sturge then propose that these terms are the principal cause of the remaining splittings: The total second-order spin-orbit coupling matrix element a is taken to be -4 to -5 cm^{-1} and a splitting of this magnitude is superimposed on the ^3A and ^3E levels. The further splitting of the upper level is then attributed to smaller first-order spin-orbit terms.

Figure 11(d) shows the energy-level diagrams obtained by including an out-of-state second-order spin-orbit matrix element varying from -2 to -8 cm^{-1}. These do not support the Scott-Sturge assignment; while the ^3E state is split by the right order of magnitude, the splitting of the ^3A level, is, for all values of a, very small. The discrepancy arises because Scott and Sturge simply added the trigonal-field and spin-orbit splittings together, instead of properly diagonalizing the combined matrix.

We are therefore obliged to reconsider the interpretation of the zero-field structure. The first possibility is that the numerical magnitudes of the various terms have been incorrectly chosen. The trigonal-field terms cannot be appreciably increased, since then the over-all splitting would become larger than observed. Within the framework employed by Scott and Sturge, the first-order spin-orbit coupling terms therefore cannot be raised either, since it is assumed that all off-diagonal perturbations are equally quenched. The possibility that first-order spin-orbit effects could be significant is thereby eliminated. The only other terms of any magnitude are the diagonal second-order spin-orbit coupling terms. The search then reduces to consideration of reduced trigonal-field terms and a greater variety of diagonal second-order spin-orbit contributions. A survey of the energy diagrams obtained over a wide range of relative values of the matrix elements a and b, including both positive and negative values for a, shows that, with these terms alone, it is not possible to even approach a reasonable fit to the observed pattern. As a last resort it might be suggested that some of the parameters used in evaluating matrix elements are incorrect. However, it would require very substantial changes to make much difference to the above conclusions and errors of this magnitude seem unlikely.

We are thus forced to the conclusion that a basic modification of the Scott-Sturge model is necessary to accomodate the experimental data. This might either be sought in the direction of a less restricted semi-empirical model or involve a jump to a more rigorous approach. For the present we would like to preserve as much of the Scott-Sturge model as possible. Therefore, and also because it is simpler, the former approach is taken up first. The aim is, then, to change the model in such a way as to allow a very different energy-level diagram to be obtained without drastically affecting the general qualitative picture.

The easiest way to achieve this is to postulate that the first-order spin-orbit coupling is in fact contributing significantly to the observed splittings. This in turn requires it to be less quenched than in the trigonal field. In view of the approximate nature of the model, particularly in its treatment of the trigonal field, there is no real reason to expect that all first-order quenching factors should be identical. If we also assume that, as before, in the second-order matrix only the diagonal spin-orbit and purely trigonal-field terms are significant, we can then take the $^3T_{2g}$ matrix to be of the general form shown in Fig. 10 [part (e) of caption], where, with the abolition of equal quenching, the parameters s, t, and x are independent. The procedure is now to vary s, t, and x in quest of sets of values providing a resonable fit to the data. No restrictions are imposed except that s and t be of the same sign as in the Scott-Sturge model; x is allowed both positive and negative values since the theoretical estimates could be in error. In selecting acceptable level schemes we at first require only that the degeneracies demonstrated by Zeeman splittings be reproduced. Thus, levels 2, 4, and 5 must be degenerate (though conceivably accidentally so). Levels 1 and 3 may be degenerate or nondegenerate; if both are nondegenerate, the location of the remaining ninth level is not restricted.

A study of the results obtained over the whole range of parameter values leads to the conclusion that a correct ordering of levels and reasonable relative spacings are obtainable in three regions of parameter space. Examples of each, labelled A, B, and C, are exhibited in Fig. 12 alongside the experimental energy levels. The diagrams were derived by guessing optimum relative values for s, t, and x from our survey calculations and then scaling the parameters to give a total energy spread equal to the observed value of 14 cm^{-1}. In A, levels 3 and 4 are genuine and accidental doublets, respectively. B makes level 3 a singlet and level 4 an accidental triplet. C requires levels 1, 3, and 4 to be doublet, singlet, and doublet, respectively and makes level 2 an accidental doublet. As they stand, A and B are in quite good agreement with the experimental spacings; C is rather farther off. The fit could be improved to some extent by adjusting the parameters. However, allowing for the approximate nature of the model and experimental uncertainties, it is clear that, from the

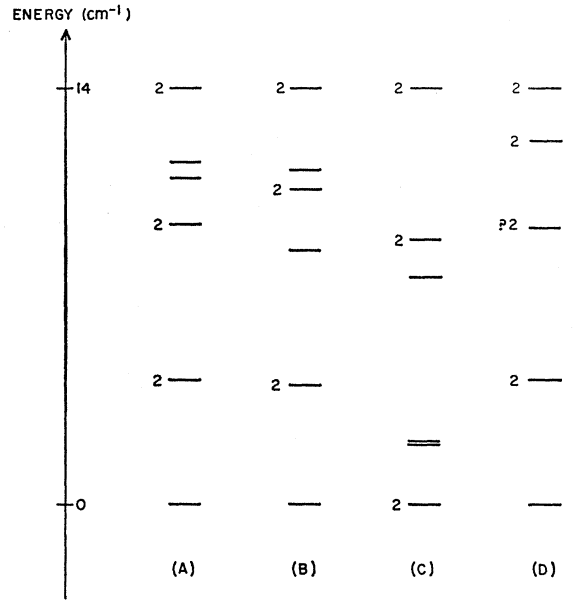

FIG. 12. Energy levels calculated from the matrix of Fig. 10 [part (e)]:A: $x=-6.931$, $t=-1.733$, $s=1.733$; B: $x=-2.935$, $t=-1.957$, $s=2.935$; C: $x=-5.488$, $t=-1.220$, $s=3.659$. D shows the experimental levels. Numbers indicate degeneracy.

zero-field energies alone, the three alternatives cannot be definitely distinguished. Therefore, nothing is to be gained by such refinements.

The three schemes are in fact quite disparate, however, differing for example in the degeneracies, and hence symmetries, assigned to levels 1, 2, 3, and 4. A distinction should therefore be possible by comparison with the observed selection rules and Zeeman patterns. Within the theoretical model elaborated above, states can be classified according to the C_3 group, singly and doubly degenerate levels belonging, respectively, to A and E representations, and C_3 selection rules should operate. Excited-state symmetries were deduced from experiment on this assumption in Sec. III. Comparison with Fig. 12 shows that A exactly reproduces these assignments while B and C are in substantial disagreement. B makes levels 3 and 4, respectively, A and $A+E$; C requires levels 1, 2, 3, and 4 to be E, $A+A$, A, and E. The selection rules thus unambiguously favor scheme A.

To calculate the Zeeman behavior, a term $\mathcal{H}_{MF}=\beta(\mathbf{L}+2\mathbf{S})\cdot\mathbf{H}$ is added to the Hamiltonian, where β is the Bohr magneton. $2\beta\mathbf{S}\cdot\mathbf{H}$ is a diagonal operator and hence is unquenched by the Jahn-Teller effect. Its matrices within the ground ${}^3T_{2g}$ vibronic state for $\mathbf{H}$ along and perpendicular to the trigonal axis (and, in the latter case, along the cubic $1\bar{1}0$ direction) are given in Fig. 10 [part (f) of caption]; they contain only first-order terms. $\beta\mathbf{L}\cdot\mathbf{H}$, on the other hand, is off-diagonal and gives rise to a quenched first-order matrix and a nonzero second-order matrix, the latter including cross terms with $\mathcal{H}_{so}$ and $\mathcal{H}_{TF}$. Calculation of the magnitudes of these elements, however, shows none over 0.1 cm^{-1} at 100 kG. For practicable fields, therefore, the $\mathcal{H}_{MF}$ matrix can be adequately approximated by that of $2\beta\mathbf{S}\cdot\mathbf{H}$.

The Zeeman pattern for scheme A is shown in Fig. 13. All qualitative features of the $\mathbf{H}\parallel c$ behavior are reproduced: levels 2, 4 (an accidental doublet), and 5 split appreciably, levels 4 and 5 about equally; level 3 (truly degenerate) does not split but increases slightly in energy; level 1 goes down in energy and the rise of the upper component of level 2 reverses at $\sim$30 kG. The $\mathbf{H}\perp c$ spectrum is almost as satisfactory: Except for level 3, no appreciable splittings are predicted and the energy trends are all of the form observed. The splitting of level 3 can either be supposed unresolved in the spectrum, because it is less than the linewidth of $\sigma 5$, unobserved owing to selection rules, or a result of an inadequate theoretical model. Any or all of these explanations might be valid to some extent; we shall discuss the second in more detail later. The quantitative agreement with experiment is in all cases good, too, if the preferred smaller splitting of level 2 with $\mathbf{H}\parallel c$ is the correct one, both shifts and splittings being within $\sim$1 cm^{-1}. The experimental errors are probably a substantial fraction of 1 cm^{-1} and similar variations are likely to occur with refinement of the theoretical parameters.

The Zeeman behavior of alternatives B and C has also been calculated. C is definitely inconsistent with

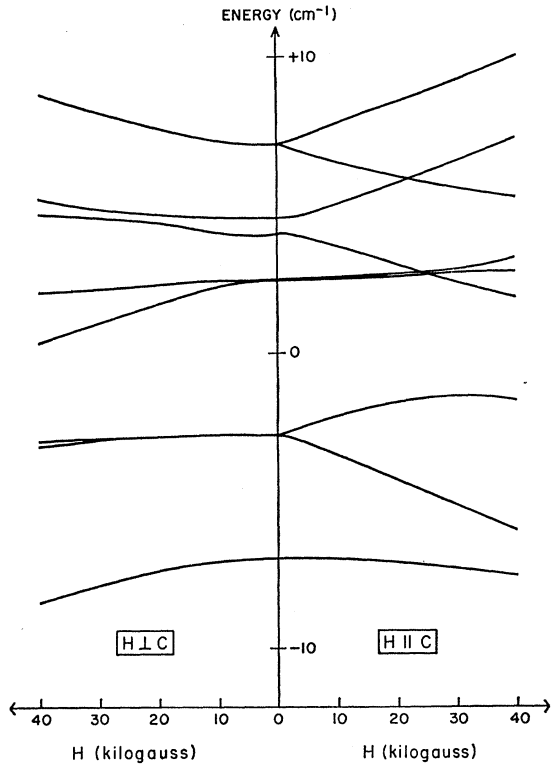

FIG. 13. Zeeman behavior calculated for $\mathbf{H}\parallel c$ and $\mathbf{H}\perp c$ and $x=-6.931$, $t=-1.733$, $s=1.733$.

the data since the lowest level is predicted to split by ~ 5 cm^{-1} in a field of 40 kG $\|$ c. Alternative B successfully predicts the gross over-all features of the $\mathbf{H} \| c$ data if it is supposed that only the highest and lowest of the three Zeeman components of level 4 are observed. Some of the finer details are not correct; level 3 is predicted to decrease in energy and the upper component of level 2 does not flatten out as $\mathbf{H}$ increases. With $\mathbf{H} \perp c$, a threefold splitting of level 4 is calculated, greater than that with $\mathbf{H} \| c$. To bring this in line with experiment it is again necessary to postulate favorable selection rules, in this case such that the lowest component is not observed. The remaining features are not wildly inconsistent with the observed spectra. Thus, adoption of this scheme would require some rather arbitrary assumptions and a disregard for small discrepancies.

The observed selection rules and Zeeman behavior thus together eliminate two of the three alternatives and agree very satisfactorily with scheme A. It then remains to ask whether the model, with these parameters, also predicts the experimental intensities. The 0-0 $^3T_{2g}$ band is electric-dipole allowed via the trigonal field. Although it is adequate to take the $^3T_{2g}$ states as pure d^n functions in the energy calculations, it is therefore necessary for intensity estimates to take account of this perturbation in the wavefunctions. Following McClure[10] we assume that spin-orbit mixing of different terms is not important and write

$$\begin{aligned}
|\xi' M_S\rangle &= (\tfrac{1}{3}\sqrt{3})\,|A' M_S\rangle - (\tfrac{1}{6}\sqrt{6})\,|E_x' M_S\rangle \\
&\quad + (\tfrac{1}{2}\sqrt{2})\,|E_y' M_S\rangle, \\
|\eta' M_S\rangle &= (\tfrac{1}{3}\sqrt{3})\,|A' M_S\rangle - (\tfrac{1}{6}\sqrt{6})\,|E_x' M_S\rangle \\
&\quad - (\tfrac{1}{2}\sqrt{2})\,|E_y' M_S\rangle, \\
|\zeta' M_S\rangle &= (\tfrac{1}{3}\sqrt{3})\,|A' M_S\rangle + (\tfrac{1}{3}\sqrt{6})\,|E_x' M_S\rangle, \qquad (12)
\end{aligned}$$

where the primes denote perturbed functions and $|A\rangle$, $|E_x\rangle$, and $|E_y\rangle$ transform as z, x, and y in the trigonal coordinate system, x being along the cubic $1\bar{1}0$ direction. The ^3A ground state is similarly now taken as a perturbed function $|^3A_0'\rangle$. The required matrix elements of the electric dipole operator $\mathfrak{y}$ are of the form $\langle \Gamma_0' v_0 | \mathfrak{y} | \sum_i c_i \Gamma_i' v_i \rangle$, where Γ_0' and Γ_i' specify perturbed ^3A and $^3T_{2g}$ states, v_0 and v_i their associated vibrational functions, and the coefficients c_i generate an eigenfunction of the energy matrix. Adopting the Franck-Condon approximation then gives

$$\langle \Gamma_0' v_0 | \mathfrak{y} | \sum_i c_i \Gamma_i' v_i \rangle = \sum_i c_i \langle \Gamma_0' | \mathfrak{y} | \Gamma_i' \rangle \langle v_0 | v_i \rangle. \qquad (13)$$

In the Scott-Sturge model, the vibrational states are those of an undistorted VO_6 octahedron; in this case, by symmetry, $\langle v_0 | v_i \rangle$ is a constant, independent of i.

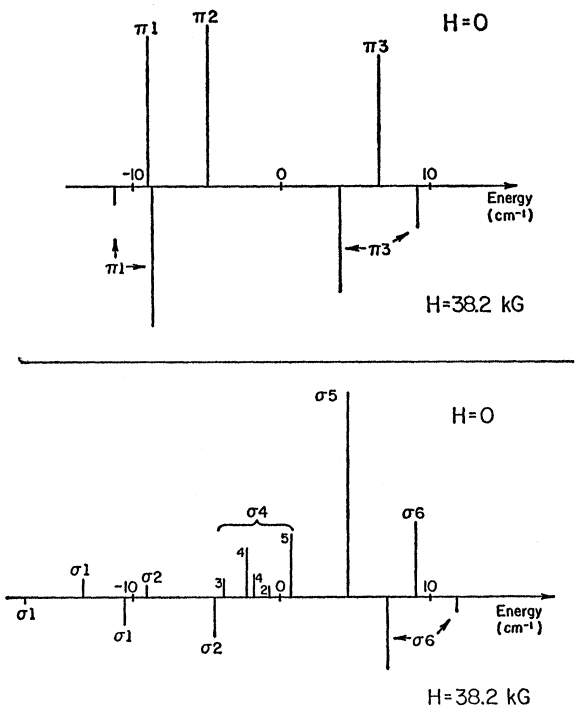

FIG. 14. Relative electric dipole intensities calculated for $H=0$ and $\mathbf{H} \| c = 38.2$ kG, 10°K and $x=-6.931$, $t=-1.733$, $s=1.733$. For clarity the 38.2-kG spectra include only Zeeman components of transitions observed to split. Other lines show only minor changes in intensity from the zero-field spectrum. Numbers attached to $\sigma 4$ transitions specify the excited levels involved.

Then

$$\langle \Gamma_0' v_0 | \mathfrak{y} | \sum_i c_i \Gamma_i' v_i \rangle \propto \langle \Gamma_0' | \mathfrak{y} | \sum_i c_i \Gamma_i' \rangle. \qquad (14)$$

The π and σ intensities are determined by matrix elements of μ_z and μ_y, respectively, where $z \| c$ and y is chosen to be the σ polarization direction. From group theory we have

$$\begin{aligned}
&\langle A_0' M_S | \mu_z | A' M_S' \rangle = \pi \delta_{M_S, M_S'}, \\
&\langle A_0' M_S | \mu_x | E_x' M_S' \rangle = \langle A_0' M_S | \mu_y | E_y' M_S' \rangle \\
&\qquad = \sigma_1 \delta_{M_S, M_S'}, \\
&\langle A_0' M_S | \mu_x | E_y' M_S' \rangle = -\langle A_0' M_S | \mu_y | E_x' M_S' \rangle \\
&\qquad = \sigma_2 \delta_{M_S M_S'}, \qquad (15)
\end{aligned}$$

where, by suitable phase choice, π, σ_1, and σ_2 can be chosen to be real. Substituting Eq. (12) into Eq. (14), transforming spin functions from cubic to trigonal axes, and using Eq. (15) then allows intensities to be calculated in terms of π, σ_1, and σ_2.

The results of such calculations for scheme A in zero field and 38.2 kG $\|$ c at 10°K are shown in Fig. 14.[32] The agreement with experiment (Figs. 1–5) is clearly

[32] Note that for $\mathbf{H} \| c$, σ intensities depend only on $\sigma_1^2 + \sigma_2^2$. Hence, relative σ intensity predictions do not require relative values of σ_1 and σ_2.

very satisfactory. The strongest transitions predicted are those observed. Hot transitions to levels 4 and 5 are both predicted to be strong, supporting the assignment of $\sigma 4$ to both.[33] The observed intensity differences of Zeeman components stemming from the same zero-field transition are also correctly reproduced: the upper components of $\pi 1$, $\sigma 1$, and $\sigma 2$ are stronger than the lower, while the reverse holds for $\pi 3$ and $\sigma 6$. Since no splittings or dramatic intensity changes are seen with $\mathbf{H} \perp c$, results are not given for this case. However, the intensities of the $\sigma 5$ Zeeman components are of interest since a splitting of level 3 was calculated but not observed. In the $\mathbf{H} \perp c$ experiment the light is polarized perpendicular to both $\mathbf{H}$ and the c axis. For this case it turns out that the intensity of the upper Zeeman component is determined by σ_2 alone and that of the lower by just σ_1. Then if σ_1 and σ_2 are of very unequal magnitude, only one transition will be seen. The observed Zeeman shift agrees well with our calculation if the lower transition is being detected. Hence, the discrepancy can be removed by assuming $\sigma_1 \gg \sigma_2$.[34] For light polarized along $\mathbf{H}$, the selection rules are reversed, and, with $\sigma_1 \gg \sigma_2$, the upper Zeeman component should then dominate. Unfortunately, we were not able to carry out this experiment.

The oscillator strength of the whole ${}^3A \rightarrow {}^3T_{2g}$ band arising from magnetic-dipole transitions polarized along axis α can be calculated from the expression[35]

$$f = (\nu/6\hbar mc^2) \sum_{i,M_S,M_S'} \sum |\langle {}^3A, M_S \mid L_\alpha \mid {}^3T_{2g}, iM_S' \rangle|^2. \quad (16)$$

Substituting strong-field d^2 functions and ignoring any reduction of orbital angular momentum by covalency effects, we obtain f values of 8×10^{-6} and 2×10^{-6} for parallel and perpendicular polarizations, respectively. McClure[10] gives $f_\sigma = 3.6\times10^{-5}$ and $f_\pi = 2.8\times10^{-5}$ for the total ${}^3T_{2g}$ oscillator strengths. The calculation thus suggests an appreciable magnetic-dipole contribution to the σ intensity. Assuming the same ratios to apply to the 0-0 band, it is consistent with our identification of magnetic dipole intensity in the σ spectrum.

The relative intensities of parallel-polarized magnetic dipole transitions predicted from parameter set A are the same as for parallel-polarized electric dipole transitions (Fig. 14) since the electric and magnetic dipole operators transform identically in C_3. All three π transitions are hence expected to occur in the σ spectrum as magnetic dipole transitions with roughly equal intensity. Since $\sigma 2$ is allowed in both polarizations, however, its magnetic-dipole contribution cannot be determined. The $\pi 3$ transition would also be indistinguishable in the σ polarization owing to the considerable intensity of $\sigma 5$ and $\sigma 6$ in that region. $\sigma 3$ is thus the only transition expected to be both strongly and identifiably magnetic dipole in origin— and this is our observation.

A matrix of the form of Fig. 10 [see part (e) of caption] together with parameters close to $s = 1.733$, $t = -1.733$, $x = -6.931$ thus leads to a very satisfactory account of the 0-0 ${}^3T_{2g}$ $Al_2O_3:V^{3+}$ spectrum and its Zeeman effect. It is not possible to show that this matrix is unique in this respect. However, it appears to be the only matrix of this form (with s positive and t negative) capable of providing such over-all agreement. It is therefore the only matrix which allows the principal features of the Scott-Sturge model to be retained. The actual numerical changes from the Scott-Sturge matrix are quite small: The trigonal-field splitting is roughly halved and the first-order spin-orbit terms about doubled. The ratio $s:t$ thus increases approximately fourfold and the quenching factors for the first-order spin-orbit coupling and trigonal field become $\sim$0.04 and $\sim$0.01. Compared to the over-all quenching this difference is relatively minor. In this connection, it is mildly satisfying that, of the three alternative assignments conceived in Fig. 12, that ultimately proving most satisfactory involves the least drastic change in $s:t$. The other modification of the complete Jahn-Teller matrix [Fig. 10, sum of parts (b), (c), and (d) of the caption] made in Fig. 10 [part (e)] was the neglect of off-diagonal second-order spin-orbit and cross terms. Such terms are not totally insignificant. However, with the removal of equal quenching, it is no longer possible to calculate them meaningfully. A calculation using the larger quenching factor for these elements showed minor changes, of the same order as the deviations from experiment. As mentioned before, variation of the parameters s, t, and x would probably allow an improved fit to experiment to be obtained. However, given both experimental and theoretical uncertainties such a procedure would be of questionable significance and has not been attempted.

The success of the theoretical model vindicates the empirical assignments of the spectrum made in Sec. III. In particular, it is now clear that $\sigma 4$ cannot involve an otherwise unobserved, degenerate upper state, since this would raise the number of levels above nine—the maximum permitted by the model.

V. CONCLUSION

The primary conclusion arrived at is that Ham's model calculations serve successfully as a basis for interpreting the behavior of the $Al_2O_3:V^{3+}$ ${}^3T_{2g}$ band. This generates confidence in their increasing application to the spectra of ions in crystals. As a corollary, however, it has been found that Ham's quantitative results must be taken over with some flexibility: In $Al_2O_3:V^{3+}$, it is not possible to maintain equal quenching

[33] A significant intensity is also predicted for the hot transition to level 3, which should lie between $\sigma 3$ and the $\sigma 4$ maximum. This may be responsible for the shoulder observed in this region in the axial spectrum (Fig. 5).

[34] If the site symmetry were C_{3v} instead of C_3, σ_1 would be zero. This assumption therefore leads to the conclusion that the distortion from C_{3v} is the dominant contributor to the intensity. This supposition is also necessary to account for the existence of the π spectrum.

[35] Ref. 27, p. 290; note that this expression is unaffected by first-order Jahn-Teller interactions.

for the trigonal-field and spin-orbit perturbations. This presumably arises from the improper treatment of the trigonal field as a purely electronic perturbation on an octahedral system. An *a priori* calculation without this deficiency would be of great interest and is currently under consideration.[35a] Such deviations from the model results may well prove to be of general occurrence. As yet, the ground states of $Al_2O_3:Ti^{3+}$ and $Al_2O_3:V^{4+}$ appear to be the only other systems with more than one quenched perturbation that have been analyzed and here the available magnetic resonance and far-infrared data have been interpreted with equal quenching.[36] Of course, to detect such effects requires a fairly precise knowledge of the splittings expected in the absence of the Jahn-Teller effect. In this respect we have been fortunate in having Macfarlane's ligand-field calculations for $Al_2O_3:V^{3+}$ at hand.

Returning to the specific $^3T_{2g}$ $Al_2O_3:V^{3+}$ problem, experiments to further test our model would be of interest. Two in particular are worth mentioning, namely, Zeeman experiments at higher fields and circular polarization and dichroism studies. The calculated behavior of the $^3T_{2g}$ manifold becomes quite complicated immediately above 50 kG and experiments in the 50–100-kG region would provide a very stringent test of predictions. At much higher fields, the magnetic-field perturbation becomes dominant and the pattern simplifies, as illustrated in Fig. 15. $\mathcal{H}_{MF}$ splits $^3T_{2g}$ into three threefold degenerate states, each degenerate set having the same value (+1, 0, or −1) of the spin component M_S along the magnetic field ($\| c$ in Fig. 15) and comprising the three orbital components. $\mathcal{H}_{so}$ and $\mathcal{H}_{TF}$ then produce small splittings of the orbital degeneracies. The ^3A ground state behaves similarly. A specific case of particular interest in this region is with a field $\| c$ sufficiently large that the $M_S=-1$ ^3A state alone is populated. Then if M_S is conserved in a transition, as assumed in the intensity calculations of the previous section, only the three $M_S=-1$ excited states would be observed; with C_3 selection rules these would give one π and two σ-polarized transitions. Transforming the matrix of Fig. 10 [see part (e) of caption] to an $M_S=+1$, 0, −1 representation, it turns out that s and t alone, and not x, contribute to the first-order splitting of an M_S triplet. Hence this experiment would allow more precise values of s and t to be obtained.

Measurements of the circular polarization and dichroism created by the field can be carried out with light propagating along the trigonal axis and hence for perpendicularly polarized bands. The selection rules for left (L) and right (R) circularly polarized transitions in C_3 are:

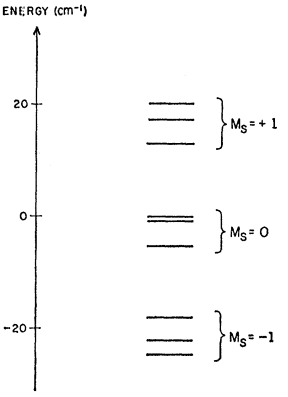

FIG. 15. Zeeman pattern calculated for $\mathbf{H}\|c=200$ kG and $x=-6.931$, $t=-1.733$, $s=1.733$. M_S values refer to the trigonal axis.

$$\overset{L}{A\rightarrow E_+} \qquad \overset{L}{E_+\rightarrow E_-} \qquad \overset{R}{E_+\rightarrow A}$$

$$\overset{R}{A\rightarrow E_-} \qquad \overset{R}{E_-\rightarrow E_+} \qquad \overset{L}{E_-\rightarrow A}.$$

Each Zeeman component is predicted to be completely circularly polarized. Experiments using a single circular polarization would thus provide further information on the validity of the C_3 selection rules and check the symmetry assignments of individual upper-state Zeeman levels. Also, since several transitions would thereby be eliminated from the spectrum, a better identification of those remaining would be permitted and previously hidden bands possibly also brought to light. Magnetic circular dichroism measurements would lead to similar information but, in addition, could also definitely prove the degeneracy of $\sigma 5$. If our assignment is correct the relative displacement of the oppositely polarized Zeeman components, although unobservably small in pure linearly or circularly polarized spectra, would lead to a dichroism changing in sign on dispersion through $\sigma 5$, unless the splitting is so small that dichroism arising from field-induced intensity changes (of like sign for both Zeeman components) is completely dominant. If $\sigma 5$ is actually nondegenerate, the dichroism must be of the same sign throughout the band. The direction of a change in sign, if observed, would also further check our calculation, since this predicts the component of higher energy to be L-polarized.

ACKNOWLEDGMENTS

We would like to express our gratitude to Professor D. S. McClure for his support of this work and for continual advice and encouragement; to K. Klump, J. Wessel, E. Zalewski and, especially, R. Meltzer for generous technical assistance; to Dr. S. A. Marshall for the loan of the crystal; to Dr. M. D. Sturge for providing copies of papers prior to publication; and to Professor O. Schnepp for an invaluable discussion.

[35a] *Note added in proof:* We have now shown that, by modifying Ham's calculations to take explicit account of the trigonal distortion, the unequal quenching of the trigonal-field and spin-orbit splittings can be simply and satisfactorily explained. This work will shortly be submitted for publication.

[36] R. M. Macfarlane, J. Y. Wong, and M. D. Sturge, Phys. Rev. **166**, 250 (1968). This paper uses Ham's results in a simliar manner to the present work. It is not clear, however, that the use of perturbation theory is valid in the case of the Ti^{3+} and V^{4+} $^2T_{2g}$ states since the splittings are of the same order of magnitude as the vibrational frequencies. Further discussion of this point is desirable.